

# Analog Signal Performance of a Hollow-Core-Waveguide using High-Contrast-Gratings

H. Huang<sup>1</sup>, Y. Yue<sup>1</sup>, L. Zhang<sup>1</sup>, X. Wang<sup>1</sup>, C. Chase<sup>2</sup>, D. Parekh<sup>2</sup>, F. Sedgwick<sup>2</sup>, M. Tur<sup>3</sup>, M. C. Wu<sup>2</sup>, C. J. Chang-Hasnain<sup>2</sup> and A. E. Willner<sup>1</sup>

1. Department of Electrical Engineering, Univ. of Southern California, Los Angeles, CA 90089, USA, Email: haoh@usc.edu

2. Department of Electrical Engineering and Computer Sciences, Univ. of California, Berkeley, CA, 94720, USA

3. School of Electrical Engineering, Tel-Aviv University, Tel-Aviv, 69978, ISRAEL

**Abstract:** On-chip analog signal performance of high-contrast-grating hollow-core-waveguide is evaluated. SFDR of >100 dB can be achieved for IM3 over a wide RF frequency range of 80 GHz and optical wavelength band of 50 nm after a 100-m propagation. An optimal waveguide design can produce analog performance comparable to optical fibers, which is dramatically better when compared with integrated low-loss silicon waveguides.

**OCIS codes:** (050.2770) Gratings; (060.5625) Radio frequency photonics; (130.3120) Integrated optics devices

## 1. Introduction

Waveguide structures are used for many elements inside photonic integrated circuits (PICs). For microwave analog photonic links in which optical signals propagate through on-chip waveguiding structures, a key figure-of-merit is the maintenance of linearity. Hollow-core-waveguides (HW) have been shown to exhibit extremely low nonlinearity as well as low loss and high thermal stability, all important characteristics for analog elements [1]. Moreover, high-contrast gratings (HCG) have been used to confine the wave in the hollow core and have been shown to further reduce the propagation loss [2].

For a HCG with optimized design, the light propagating in the hollow region excites modes in the grating bars. The first two excited modes can cancel one another outside the gratings, which leads to extremely high reflectivity [3]. Recently, it has been shown that HCG waveguides exhibit a low nonlinearity under a wide variety of waveguide parameters [4]. However, both loss and chromatic dispersion can vary greatly and might affect the operation of an analog link or subsystem [5]. A laudable goal would be to characterize the HCG hollow-core waveguides for their suitability in microwave analog applications.

In this paper, we simulate the analog signal performance of a hollow-core-waveguide that uses high-contrast-gratings. The link spur-free dynamic range (SFDR) of the third-order inter-modulation distortion (IM3), second-order harmonic distortion (SHD) and third-order distortion (THD) are analyzed. Even after a 100-m propagation, HCG-HW can operate at modulation frequencies of up to 80 GHz, and an optical bandwidth of >50 nm, while maintaining a SHD SFDR>85 dB. The maximum SFDR achievable for IM3 is limited by the Mach-Zehnder modulator (MZM) to 109.9dB/Hz<sup>2/3</sup> [6]. The impact of fabrication tolerance of a HCG-HW on linearity is also investigated. Optimally designed HCG-HWs perform as well as single mode fiber (SMF). This is a quite promising building block for on-chip analog systems. Even with the worst case of a 20-nm fabrication variation for all the grating parameters, HCG-HWs behave better than low-loss silicon ridge waveguides.

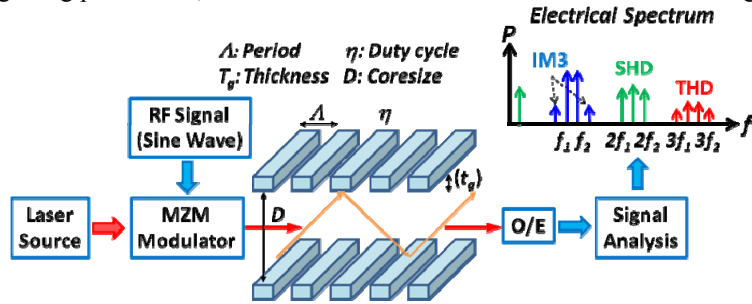


Fig. 1. Analysis model of high-index-contrast grating hollow-core waveguide in an analog link

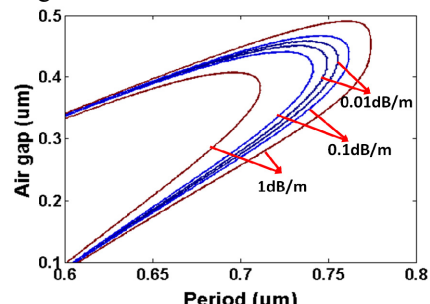


Fig. 2. Low loss range of HCG-HW with a 340-nm grating thickness

## 2. Analysis model

The analysis model is shown in Fig. 1. A continuous wave (CW) with a linewidth of 1k Hz is modulated by radio frequency (RF) signals ( $f_1=40$  GHz,  $f_2=41$  GHz) through a MZM. Relative intensity noise (RIN) and power of the CW source are assumed to be -165 dB/Hz and 100 mW, respectively. The MZM with a half-wave voltage of 5V is

### OThA3.pdf

biased at the quadrature point to use the linear portion of the raised-cosine transfer function. The modulated optical signal is then launched into the HCG-HW for signal transmission. The structure of the HCG-HW is shown in Fig.1. The HCG-HW with optimal design for low loss (Thickness: 340nm, Period: 750nm, Air gap: 0.467, Core size: 15um) has a loss of 0.0052 dB/m, dispersion of 10.9 ps/nm/km and a nonlinearity of  $6.5 \times 10^{-10}$  W/m at 1550 nm [4]. Fig.2 shows a large low-loss area of HCG-HW in the plane of period × air gap. Figure 3 also shows the low chromatic dispersion of HCG-HW for a broad wavelength range. After O/E conversion by a detector with a responsibility of 0.7 A/W, the output signal distortion is evaluated.

As SFDR is one of the most important indicators in an analog system [7], we mainly evaluate the analog signal performance of HCG-HW by analyzing the IM3 SFDR, SHD SFDR and THD SFDR. SFDR is defined as the signal to noise ratio (SNR) of RF carrier at the link output when the link input signal power is at a level that produces distortion products with their output powers equal to the output noise level [7]. Nonlinearity, dispersion and loss affect the SFDR of the link in different ways [6-10]. Dispersion induces a phase shift between the optical carrier and the sidebands, which causes distortion terms, particularly for high modulation frequencies. Fig. 4 shows that dispersion induces a periodic change in the intensity of the distortion terms with a modulation frequency of 40 GHz. The period is determined by the frequency spacing of different optical tones that generate RF carrier and distortion products after photo-detection. Since the frequency of IM3 ( $2f_1-f_2$ ) is very close to that of the RF carrier ( $f_1$ ), they have close periodicity. Consequently, the IM3 SFDR is relatively tolerant to the dispersion variation. However, SHD and THD are more sensitive to dispersion, because they have double and triple frequency spacings, respectively. The optical loss induced SFDR reduction is analyzed in [8]. Every 1dB of optical loss results in a 2dB attention of electrical power of the output signal according to square law detection. However, the consequent reduction on noise floor might be 0-2dB, depending on which kind of noise source dominates at the output. The different reductions in output signal power and noise floor will finally result in changes on SFDR. As the nonlinearity of HCG-HW is negligibly low [4], the dispersion and optical loss are the main contributors to changes in the SFDR of the link.

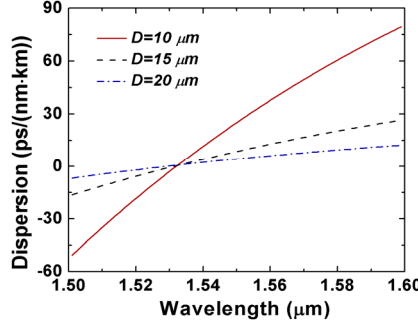


Fig. 3. Chromatic dispersion of HCG-HW with different core sizes.

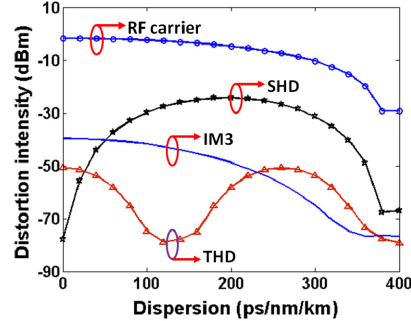


Fig. 4. Power of RF carrier and distortions as functions of HCG-HW dispersion.

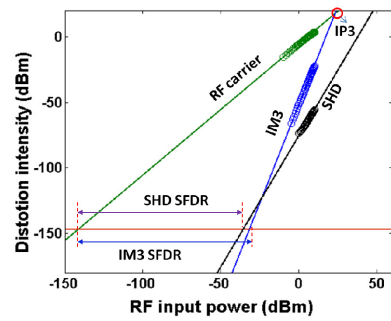


Fig. 5. Power of RF carrier and distortions as functions of RF input power

### 3. Bandwidth and SFDR limitation

Using the model described above, we obtain the IM3 and SHD SFDRs in a 100-m-long HCG-HW link under the optimal waveguide design, these are  $109.9 \text{ dB/Hz}^{2/3}$  and  $105.7 \text{ dB/Hz}^{1/2}$ , respectively, at a modulation frequency of 40 GHz, as shown in Fig.5.

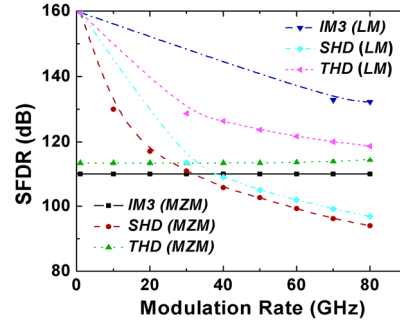


Fig. 6. SFDR as function of modulation frequency. By comparing with a linear modulation(LM) case, we find that IM3 SFDR is limited by a MZM, and SHD SFDR is limited by HCG HW dispersion.

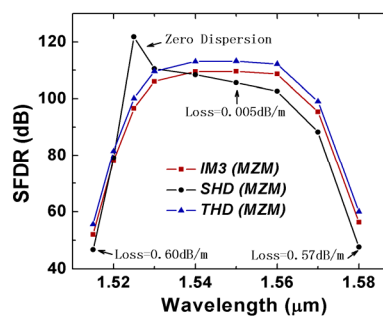


Fig. 7. SFDR as function of wavelength. HCG HW shows an optical bandwidth of 50 nm with IM3 SFDR >100dB/Hz<sup>2/3</sup> and SHD SFDR >85dB/Hz<sup>1/2</sup>.

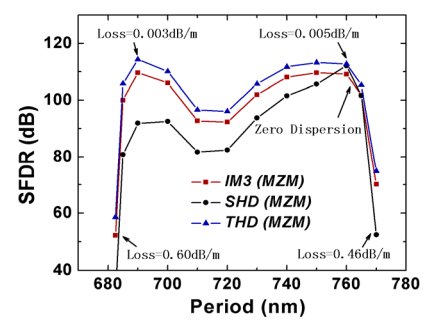


Fig. 8. SFDR as a function of grating period. Two peaks of SFDR occur at period of around 690 nm and 750 nm, which correspond to two low-loss areas.

Broadening the operational bandwidth of an analog link is of great importance. The SFDR as a function of electrical bandwidth (modulation frequency) and optical bandwidth (wavelength range) are calculated. As shown in

## OThA3.pdf

Fig. 6, IM3 SFDR remains almost a constant of  $109.9 \text{ dB/Hz}^{2/3}$ , while SHD SFDR decreases with the increasing modulation frequency, but is still greater than  $90 \text{ dB/Hz}^{1/2}$  at 80 GHz. This means that HCG-HW is promising for both sub-octave and broadband on-chip analog applications. For the optical bandwidth, as shown in Fig. 7, both SHD and IM3 have a bandwidth of  $\sim 50 \text{ nm}$  with an IM3 SFDR  $> 100 \text{ dB/Hz}^{2/3}$  and an SHD SFDR  $> 85 \text{ dB/Hz}^{1/2}$ . IM3 SFDR has a maximum value at  $\sim 1550 \text{ nm}$ , while, for SHD SFDR, the peak appears at 1525 nm, which is the zero dispersion wavelength (ZDW) of HCG.

As the real MZM itself with a raised-cosine transfer function generates nonlinear distortions, we thus calculate the SFDRs with a linear amplitude modulator to determine the contribution of the HCG waveguides to nonlinear distortion. As shown in Fig. 6, the IM3 SFDR with a linear modulator is much higher than that with a real MZM. However, analog performances are similar in terms of SHD SFDR for these two kinds of modulators. This indicates that maximum achievable IM3 SFDR is limited to  $109.9 \text{ dB/Hz}^{2/3}$  by the linearity of the MZM [6], while the achievable SHD SFDR is limited by the dispersion of HCG-HW.

### 4. Fabrication tolerance

For a waveguide with submicron gratings, the accuracy of fabrication is an important factor that should be taken into account. First, we calculate SFDR by varying only one grating parameter (period or air gap), as shown in Fig. 8 and Fig. 9. In Fig. 8, two equal peaks at period of around 690 nm and 750 nm can be found for the IM3 SFDR, while the IM3 SFDR curve is almost flat and kept at the MZM limit of  $109.9 \text{ dB/Hz}^{2/3}$  from 370 nm to 470 nm. Both of these changes are caused by optical loss. The effect of dispersion can be observed from changes in the SHD SFDR, which drops with the air gap and increases with the period. In a more realistic case, all three grating parameters (air gap, period and thickness) may change simultaneously by  $\pm 10 \text{ nm}$  to  $\pm 20 \text{ nm}$ . There are eight combinations of the three parameters (a cubic parameter space), among which the worst one (with the smallest SFDR) is taken as the lower bound of all points inside the cube. We make comparisons between the original design, and the lower bounds of a 10-nm variation and a 20-nm variation by calculating SFDR as a function of transmission distance, as shown in Fig. 10 and Fig. 11. SMF and a low-loss silicon ridge waveguide [11] are also chosen for comparison. The results show that for a propagating length of less than 1000 m, HCG-HWs with an optimal design perform as well as SMF, however, with fabrication variations both the IM3 and SHD SFDRs degrade, but even with a 20-nm variation on all three grating parameters, HCG-HWs show a much better performance when compared to a silicon ridge waveguide.

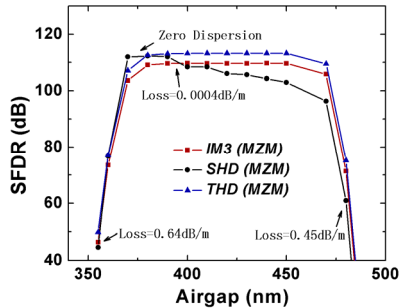


Fig. 9. SFDR as function of grating air gap. IM3 and THD SFDR are almost flat within the low loss region between 370 nm to 470 nm of air gap. SHD SFDR drops slowly with air gap due to the dispersion.

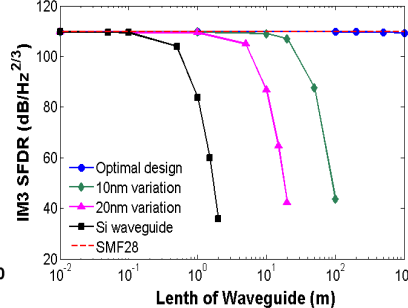


Fig. 10. IM3 SFDR as function of propagating length. A HCG HW with the optimal design performs as well as an optical fiber for 1000 m propagation. Even with 20-nm fabrication variations, HCG HW has a much higher SFDR than a silicon ridge WG.

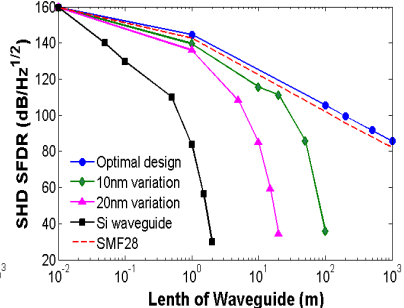


Fig. 11. SHD SFDR as function of propagating length. An optimal HCG HW performs better than SMF for  $< 1 \text{ km}$  propagation due to smaller dispersion. It is also better than Silicon ridge WGs, even with 20-nm fabrication variations.

### Acknowledgement

This work is sponsored by the Defense Advanced Research Projects Agency (DARPA) Integrated Photonic Delay (iPhoD) program (under contract numbers HR0011-09-C-0124).

### 5. References

- [1] P. Roberts, et al., Opt. Express 13, 236-244 (2005).
- [2] Y. Zhou, V. Karagodsky, B. Pesala, F. G. Sedgwick, and C. J. Chang-Hasnain, Opt. Express 17, 1508-1517 (2009).
- [3] V. Karagodsky, F. G. Sedgwick, and C. J. Chang-Hasnain, Opt. Express 18, 16973-16988 (2010).
- [4] Y. Yue, et al., OFC2010, paper OTu15.
- [5] Y. Yue, et al., IEEE Photonics Society Annual Meeting 2010, paper ThB2.
- [6] W. B. Bridges and J. H. Schaffner, IEEE Micro. Theory and Techn. , 43, 2184-2197 (1995).
- [7] C. H. Cox III, E. I. Ackerman, G. E. Betts, J. L. Prince, IEEE Trans. On Microwave Theory and Techn. 54, 906-920 (2006).
- [8] G. Katz, S. Arnon, P. Goldgeier, Y. Hauptman and N. Atias, IEE Proc.-Optoelectron., Vol. 153, No. 4, 2006.
- [9] Charles S. IH, W. Gu, IEEE Journ. On Selected Areas in Communi. , Vol. 8, 1296-1303 (1990).
- [10] G. J. Meslener, IEEE JQE, Vol. 20, 1208-1216 (1984).
- [11] R. Pafchek, R. Tummidi, J. Li, M. A. Webster, E. Chen and T. L. Koch, Appl. Opt. 48, 958-963 (2009).